RESEARCH PAPER

PCCP
www.rsc.org/pccp

Influence of hydrogen bond geometry on quadrupole coupling parameters: A theoretical study of imidazole–water and imidazole–semiquinone complexes

Jörg Fritscher

Institut für Physikalische und Theoretische Chemie and Center for Biomolecular Magnetic Resonance, Johann Wolfgang Goethe-Universität, Marie-Curie-Straße 11, D-60439 Frankfurt am Main, Germany. E-mail: j.fritscher@epr.uni-frankfurt.de

Received 10th June 2004, Accepted 30th July 2004
First published as an Advance Article on the web 25th August 2004

Density functional theory (DFT) was used to calculate electric field gradients that give rise to quadrupole couplings for nuclei with a nuclear spin $I > 1/2$. A systematic theoretical investigation of the influence of hydrogen bond geometry on ^{14}N quadrupole coupling tensors of (methyl-)imidazole is presented for the hydrogen-bonded systems imidazole–water and methylimidazole–benzosemiquinone. It reveals a strong dependence of the corresponding interaction parameters on the intermolecular arrangement, especially for the asymmetry parameter η. For both systems the largest influence on the electric field gradients was found for a variation of the hydrogen bond length r(O–N), the effects of an in- or out-of-plane distortion of the bond geometry were found to be less pronounced. Furthermore, a comparison of the ^{14}N quadrupole parameters of the hydrogen-bonded models with those of free (methyl-)imidazole allowed a characterization of specific hydrogen bonding interactions to the amino group of imidazole or histidine. Finally, the implications of the presented studies for the interpretation of experimental quadrupole coupling data of biologically relevant semiquinone–histidine systems, as *e.g.* found in bacterial reaction centres or photosystem II, are discussed.

1. Introduction

Magnetic resonance spectroscopic techniques such as electron nuclear double resonance (ENDOR) or electron spin echo envelope modulation (ESEEM) as well as nuclear quadrupole resonance (NQR) and nuclear magnetic resonance (NMR) can provide nuclear quadrupole coupling (QC) tensor eigenvalues that contain valuable information about the electrostatic environment and bonding situation of the interacting nuclei.[1,3] It should be noted that the methods based on electron paramagnetic resonance (EPR) like ENDOR and ESEEM require paramagnetic systems and furthermore solely allow a determination of the QC tensors of nuclei which show a non-negligible hyperfine coupling. However, due to various reasons, *e.g.* lack of single crystals, overlap of spectral lines or line broadening effects, it is often not possible to extract all the spectral information, to assign all coupling constants to the different interacting nuclei or to relate relative tensor orientations to the molecular frame. Furthermore, it is very difficult to directly correlate the experimental quadrupole coupling parameters with molecular structure. It has been shown in various computational studies that density functional theory (DFT)[4] calculations are capable of predicting such QC tensors for different nuclei and molecules.[5,22] These results demonstrate the reliability of the theoretical predictions and suggest that quantum chemical calculations can be the missing link between magnetic resonance data and molecular structure even for larger systems of biological relevance.

Hydrogen bonding plays a crucial role in structural and functional aspects of many biologically relevant systems.[23] The hydrogen bonding interactions may strongly influence the observed QC parameters of the involved nuclei and thus a deeper understanding of the dependence of these parameters on hydrogen bond geometry is required. While it is difficult to investigate such a systematic structure–property relationship experimentally, theoretical approaches can be very helpful to gain further insight. In order to estimate the effect of hydrogen bond geometry changes on QC parameters the system imidazole–water was chosen as a model in this work. As the side chain of the amino acid histidine, the five-membered heterocycle imidazole is a component of many proteins and therefore of widespread biological importance. Histidine residue side chains are common ligands in biological systems and form binding sites for metal ions like manganese in concanavalin A,[24] copper in galactose oxidase,[25] heme iron in cytochrome *c* peroxidase,[26,27] non-heme iron in bacterial reaction centres (bRCs)[28] or photosystem II (PSII),[29] for the diferric cluster of class I RNR,[30] for iron–sulfur clusters in the Rieske iron–sulfur protein[31] as well as for quinones, *e.g.* in bRCs[28] or PSII.[29] For that reason, methylimidazole–benzosemiquinone complexes were chosen here for systematic studies that are relevant for biological systems and may also be applied to current problems in structure determination of quinone binding sites.

So far, geometry-induced QC tensor changes have only been investigated systematically in a few studies.[11,15,17,19,21,22,32,33] In these works the dependence of QC parameters on the Fe–O–O angle in oxyheme model complexes,[11] on the Fe–N–O bond geometry in NO heme model compounds,[19] on Fe–Fe–S–H dihedral angles in [2Fe-2S*](SH)$_4$ systems,[21] on the protein backbone conformation in α-helix and β-sheet protein fragments,[15] on the hydrogen bond geometry in benzosemiquinone–water systems,[22] on the structure of ammonia–water[17] or formaldehyde–water[32] complexes as well as on the imidazole ring orientation in vanadyl–imidazole complexes[33] was investigated. However, these systems represent a different type of hydrogen bonding than the imidazole–water and methylimidazole–benzosemiquinone models or do not involve hydrogen bonding at all.

DOI: 10.1039/b408764j

In the present work a systematic investigation of the influence of hydrogen bond geometry on imidazole ^{14}N QC parameters is presented. The effects of hydrogen bond length variation and of in- and out-of-plane distortions of the bonding geometry as well as a twist of bonding partners with respect to each other are discussed and the magnitude and direction of the corresponding QC tensor changes are pointed out.

2. Theoretical background and computational details

Quadrupole coupling tensor

The QC tensor $\hat{Q}$ is a traceless tensor describing the interaction of a nuclear electric quadrupole moment Q_N due to a non-spherical nuclear charge density (for $I > 1/2$) with the electric field of the surrounding electrons.[1] Its matrix elements are defined as:[34]

$$Q_{ij}(\mathrm{N}) = \frac{eQ_\mathrm{N}}{2I_\mathrm{N}(2I_\mathrm{N}-1)h} V_{ij}(\mathrm{N}), \qquad (1)$$

where V_{ij} are the components of the electric field gradient (EFG) tensor. Based on the EFG tensor one can define the QC constant (QCC) χ and the asymmetry parameter η as

$$\chi(\mathrm{N}) = \frac{eQ_\mathrm{N}V_{zz}(\mathrm{N})}{h} \text{ and } \eta(\mathrm{N}) = \frac{V_{xx}(\mathrm{N}) - V_{yy}(\mathrm{N})}{V_{zz}(\mathrm{N})} \qquad (2)$$

with $|V_{zz}| \geq |V_{yy}| \geq |V_{xx}|$. The value of η lies between 0 and 1 and in the case of axial symmetry one obtains $|V_{xx}| = |V_{yy}|$ and $\eta = 0$. As the EFG tensor is traceless, χ and η are sufficient to fully describe the tensor in its principal axis system. For the calculations of the QCCs a standard nuclear quadrupole moment of $Q(^{14}\mathrm{N}) = 2.044(3)$ fm^2 was used.[35,36] As in many other studies[5,7,15,22] the nuclear quadrupole moments were not calibrated for the applied theoretical methods. Using the above mentioned values for Q it was possible to calculate the QCCs directly from the V_{zz} eigenvalues of the EFGs obtained from the computations.

Computational details

All calculations in the present study were carried out using standard methods and basis sets as implemented in the GAUSSIAN 98[37] program package. For the geometry optimizations as well as calculations of EFG tensors, a combination of Becke's three parameter hybrid functional B3[38] and of Perdew and Wang's correlation functional PW91[39,40] was applied. As a basis set for the imidazole–water computations 6-311+G(df,pd) was selected. This choice of the model B3PW91/6-311+G(df,pd) for geometry optimizations and property calculations was justified by the results of recent QC tensor calculations[12] on a large set of small nitrogen-containing molecules and by own studies comparing various theoretical methods (data not shown here). For the methylimidazole–benzosemiquinone system the smaller 6-31G(d) basis was chosen due to the increased computational demands of the larger complexes. The influence of the smaller basis set was checked and it was found not to be significant for this systematic study. Furthermore, it was shown recently that the 6-31G(d) basis set may be very suitable for the calculation of EFGs with DFT methods.[18] All calculations on the diamagnetic imidazole–water system were performed using restricted Kohn–Sham theory, for the paramagnetic semiquinone the unrestricted formalism was applied. To avoid errors introduced by spin contamination artefacts the $\langle \hat{S}^2 \rangle$ value was checked for all unrestricted computations and the deviations from the theoretical value were found to be sufficiently small (about 0.01).

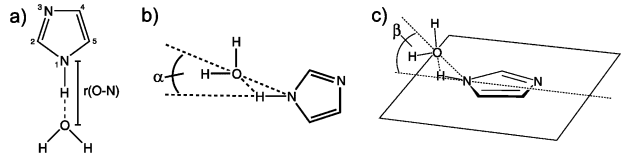

Fig. 1 Definition of the atom numbering scheme and geometric variables for the imidazole–water complexes: (a) shows the hydrogen bond length r(O–N), (b) the in-plane hydrogen bond angle α and (c) the out-of-plane hydrogen bond angle β.

3. Results and discussion

Imidazole–water

The systematic dependence of the ^{14}N quadrupole coupling parameters χ and η on the hydrogen bond geometry described by the O–N distance r, the in-plane hydrogen bond angle β and the out-of-plane hydrogen bond angle β (Fig. 1) is investigated in this part of the work. For this purpose three series of calculations, one for each variable, were performed. In each series the variable under consideration (r, α or β) was set to a range of specific values while the other variables were held constant during all computations. All other geometrical degrees of freedom were fully optimized which is of great importance to allow the hydrogen atom of the NH group to structurally relax depending on the position of the oxygen atom. This and other rearrangements in the direct bonding environment of the imidazole nitrogen atom will have a large influence on its QC parameters. For the resulting structures the ^{14}N EFG tensors and the χ and η values were calculated as a function of r, α or β.

To compare the results of the hydrogen-bonded systems with those of a non-bonded imidazole, the QC parameters for a fully optimized isolated imidazole molecule were calculated. The corresponding values for the amino (N1) and imino (N3) nitrogens are listed in Table 1. For free imidazole one finds r(N1–H) = 1.01 Å, r(C2–N1) = 1.36 Å and r(C5–N1) = 1.37 Å. The calculated QC parameters agree well with experimental gas-phase values from microwave spectroscopy[41] (χ(N1) = 2.524/2.537 MHz, η(N1) = 0.294/0.178, χ(N3) = 4.113/4.032 MHz and χ(N3) = 0.108/0.120) whereas comparison with NQR data[42] (χ(N1) = 1.391 MHz, η(N1) = 0.930, χ(N3) = 3.220 MHz and η(N3) = 0.119) reveals considerable deviations due to additional interactions in the crystalline state. Previous theoretical studies have pointed out the importance of intermolecular hydrogen bonding in imidazole crystals for a correct computation of the NQR values.[7,14,43] The good agreement between gas-phase experimental data and the calculated QC parameters demonstrates that the applied level of theory may also yield quantitatively reliable values.

The freely optimized structure of the imidazole–water complex (water oxygen hydrogen bound to the N1–H amino group) yields η and χ values as shown in Table 1. The calculated quadrupole parameters of the imino nitrogen N3 do not change significantly compared to the free imidazole. In

Table 1 Theoretical ^{14}N QC parameters for the charge neutral states of the equilibrium structures of free imidazole, the imidazole–water complex and free histidine as calculated on the B3PW91/6311+G(df,pd) level of theory. All QC constants are in MHz

	Free Imid	Imid–H_2O	Free His
χ(N1)	+2.642	+2.169	+2.325
η(N1)	0.142	0.218	0.143
χ(N3)	+4.338	+4.304	+4.329
η(N3)	0.111	0.099	0.103

contrast, the N1 parameters are considerably affected by hydrogen bonding, the value of η increases and the value of χ decreases. These trends were also found before in experimental[41,44] or theoretical[7,14,43] studies of systems involving imidazole derivatives. The hydrogen bond geometry of this equilibrium structure can be described by $r(\mathrm{O–N})_{eq} = 2.97$ Å, $\angle(\mathrm{C2–N1–O}) = 125.8°$ and $\angle(\mathrm{C5–N1–O}) = 127.3°$. The water oxygen lies in the plane spanned by C2, C5 and N1, *i.e.* $\angle(\mathrm{C5–C2–N1–O}) = 179.9°$. For the imidazole ring none of the bond lengths change with respect to the isolated imidazole molecule. Taking the equilibrium structure as a starting point, the in-plane angle α is defined as $\alpha = 125.8° - \angle(\mathrm{C2–N1–O})$ and the out-of-plane angle β as the angle between the O–N vector and the C2–C5–N1 plane (see Fig. 1). Thus, for the equilibrium structure we obtain $\alpha_{eq} = 0°$ and $\beta_{eq} = 0°$.

First, the variation of the hydrogen bond length r(O–N) is discussed. In this case the values of α and β were fixed to a value of 0° to avoid a superposition of influences from different geometric variables. For each value of r a full relaxation of the structure was performed (keeping only r, α and β frozen). The hydrogen bond length was varied in seven steps from 2.63 to 3.21 Å leading to the dependence as depicted in Fig. 2a and b. Within this series of structures the N–H bond length varies from 1.03 Å for short hydrogen bond lengths to 1.01 Å for longer hydrogen bonds. A significant effect of hydrogen bond length variation was found for the quadrupole parameters of N1 whereas the effect on the N3 coupling parameters is negligibly small. Over the whole range of hydrogen bond length variation η(N1) varies from 0.622 to 0.111 and χ(N1) from +1.796 to +2.307 MHz. The asymmetry parameter η decreases and the QCC increases when elongating the hydrogen bond. That implies that the EFG tensor becomes more axially-symmetric (V_{xx} increases and V_{yy} decreases) and that the V_{zz} component increases.

Next, the variation of the in-plane hydrogen bond angle α in the range of 0 – 40.8° is considered while the other geometric variables are fixed at the intermediate distance r(O–N) = 2.82 Å and $\beta = 0°$. All other geometric degrees of freedom were again freely optimized. The chosen value of r(O–N) is an intermediate value, which is a little shorter than the equilibrium distance, therefore, the quadrupole parameters of N1 are different from the equilibrium values for $\alpha = 0°$; η is shifted up by about 0.13 and χ shifted down by about 0.13 MHz. However, this shift does not influence the general trend of the dependence examined. The plots of η and χ as a function of the angle α are shown in Fig. 2c and d. The value of η(N1) decreases from 0.352 to 0.097 and χ(N1) increases from +2.037 to +2.293 MHz when the hydrogen bond is bent. Again, changes for the N3 QC parameters can be neglected. The N1 EFG tensor becomes almost axially-symmetric and an elongation of the V_{zz} component can be observed during the variation of α. In the principal axis system of the N1 EFG tensor the x-axis lies approximately along the N1–H bond (depending on α), the y-axis lies in the imidazole ring plane and the z-axis lies perpendicular to this plane. Fig. 3 illustrates the reorientation of the eigenvectors and the change of the principal values of the N1 EFG tensor when increasing α from 0 to 40.8°. The tensor undergoes a rotation about the V_{zz} axis by 17° contrariwise to the rotation of the water molecule.

Finally, the dependence of the nitrogen QC parameters on an alteration of the out-of-plane hydrogen bond angle β was investigated. Here, the hydrogen bond length was not completely held fixed but varied from 2.97 to 3.03 Å due to the

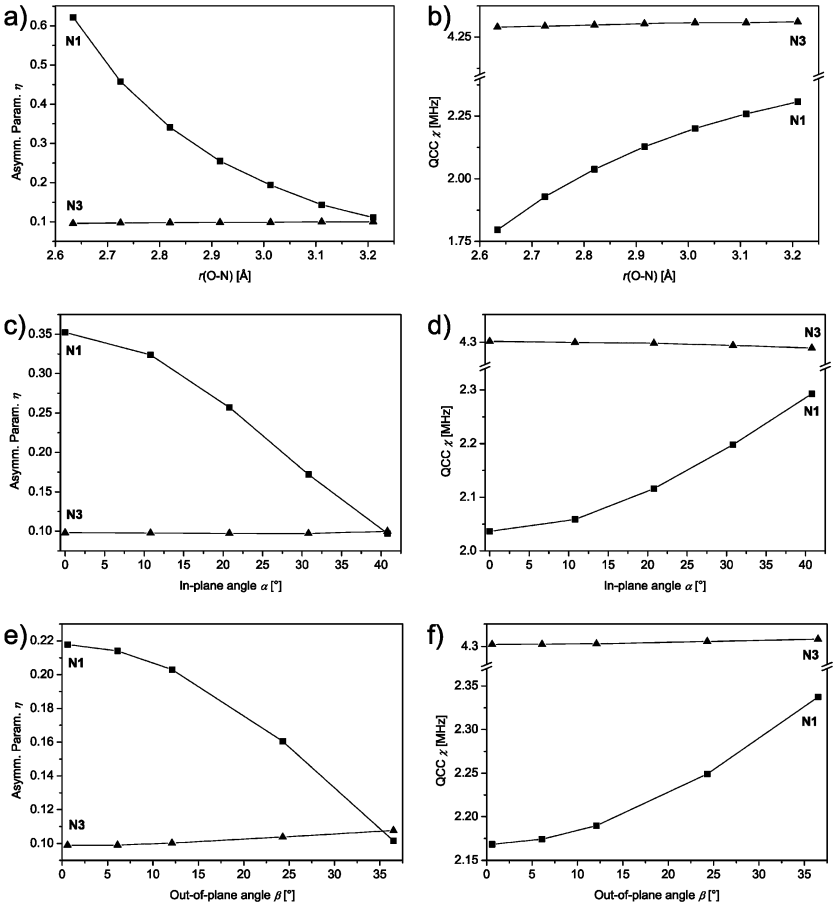

Fig. 2 Influence of the variation of the hydrogen bond length r(O–N) (a,b), the in-plane hydrogen bond angle α (c,d) and the out-of-plane hydrogen bond angle β (e,f) on the asymmetry parameters η as well as the QCCs χ of the nitrogen atoms of charge neutral imidazole–water complexes as calculated on the B3PW91/6-311+G(df,pd) level of theory.

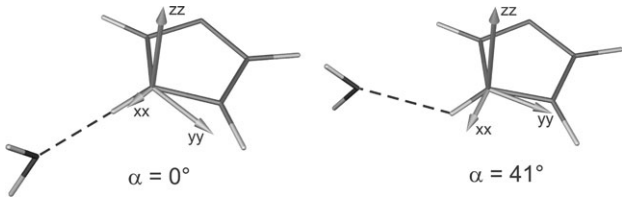

Fig. 3 Effect of in-plane hydrogen bond angle (denoted α) variation on N1 EFG tensor orientation and eigenvalues for the charge neutral imidazole–water system as calculated on the B3PW91/6-311+G(df,pd) level of theory. The arrows depict the eigenvectors of the EFG tensor scaled by the corresponding eigenvalues.

applied Z-matrix geometry specification scheme.† However, the contribution which is introduced by a bond length variation of 0.06 Å over the whole range of β values is negligible and does not alter the general trend. A constant value of 0° was chosen for the in-plane angle α during all calculations. The resulting graphs (Fig. 2e and f) reveal similar tendencies as already described for the r(O–N) and α variation. A decrease of η(N1) from 0.218 to 0.102 and an increase of χ(N1) from +2.168 to +2.337 MHz indicate a trend towards axial symmetry of the EFG tensor as well as an enlargement of V_{zz}. Additionally, the tensor undergoes a small rotation about the V_{yy} axis in the same direction as the water molecule.

For all hydrogen bond geometries investigated above, the value of χ for the hydrogen bonded amino nitrogen N1 is lower than that for the isolated imidazole molecule, whereas the value of η approaches the value for free imidazole when r, α and β are increased. However, for rather large values of r, α or β the value of η even drops below the one of the isolated imidazole. Based on these trends, it should be possible to identify imidazoles which are involved in hydrogen bonding by comparing the amino nitrogen quadrupole parameters with those of free imidazole. It is clear that in the case of a bound imidazole the QCC values will be lower and the asymmetry parameter values be higher for typical hydrogen bond geometries.[23]

A number of general statements can be made about the EFG tensor of the amino nitrogen. It approaches axial symmetry and the V_{zz} component increases as r, α or β are increased above the equilibrium values. Therefore, η tends towards zero and χ increases. The deformation or weakening of a hydrogen bond leads to an electronic situation around the nitrogen nucleus which is increasingly symmetric. When the oxygen is forced out of linearity with respect to the N1–H bond or moved further away from N1, the electric field gradient along the N1–H bond (V_{xx}) increases and approaches the value of the V_{yy} component which slowly decreases. If the hydrogen bond is shortened below the equilibrium value η increases and χ decreases. This behaviour reflects the loss of symmetry around the nitrogen nucleus as the EFG along the N1–H bond decreases significantly due to a stronger influence of the oxygen electrons.

Taking into account all these effects it can be concluded that the local surrounding of the hydrogen bonded amino nitrogen of imidazole strongly influences the QC parameters and the orientation of the EFG tensor for this atom. Therefore, the quadrupole interaction parameters are sensitive probes to detect hydrogen bonding additionally providing valuable information about the hydrogen bond geometry. Especially the asymmetry parameter η seems to be a sensitive indicator for the hydrogen bond length.

It is clear that η is influenced much more than χ for all the geometric parameters considered. The only parameter which results in an asymmetry parameter significantly larger than about 0.2 would be the length of the hydrogen bond which must be shorter than the equilibrium distance of 2.97 Å. An asymmetry parameter considerably lower than 0.2 would point towards longer hydrogen bonds as well as distortions of the bonding geometry both in- and out-of-plane.

From calculations on free histidine (applying the same theoretical model as for imidazole) the QC parameters shown in Table 1 were obtained. These values are very similar to those of free imidazole. Thus, the general trends found above may be transferred to histidines which are involved in hydrogen bonding to the amino nitrogen in a (semi-)quantitative way.

Methylimidazole–benzosemiquinone

As histidines are common hydrogen bonding partners to quinone cofactors in biological systems, *e.g.* in bRCs[28] or PSII,[29] it will be of importance to study the QC parameters of its imidazole side chain not only under the influence of a water but also of a quinone molecule. Then, it will be possible to prove a wider applicability of the trends for the imidazole–water system and obtain geometry-dependent QC data that may directly be used for the interpretation of *e.g.* ESEEM or other magnetic resonance data and thus aid in the determination of the hydrogen bonding situation of quinones. As only paramagnetic states are accessible to electron spin resonance methods, the benzosemiquinone anion radical was chosen as a hydrogen bonding partner for methylimidazole. The benzosemiquinone–methylimidazole system is supposed to be a good model for quinone binding pockets containing histidines as ligands. A representation of its structure and numbering scheme can be found in Fig. 4a. To cover a broad range of hydrogen bonding geometries various combinations of different values of the bond length r(O–N) and the angles α and β were used. Additionally, the twist angle φ (Fig. 4b) between the ring planes of the methylimidazole and the benzosemiquinone was varied. Similar to the imidazole–water system these four geometric parameters were set to a certain value for each calculation and then held fixed while all other structural degrees of freedom were optimized. The different model geometries (**Q1**–**Q11**) together with the calculated χ and η values as well as the QC parameters for free methylimidazole are listed in Table 2.

When comparing the QC parameters of the amino nitrogen N1 of free and bound methylimidazole it can be seen that the QCC χ is always smaller and the asymmetry parameter η always larger (except for η for the bond length of 3.25 Å in **Q4**) in the bound case. Thus, again it is possible to identify hydrogen bonding to the amino nitrogen just by comparison with the values of the non-bonded species. The largest deviations from the free methylimidazole values occur for very short bond lengths (**Q1**, **Q2** and **Q11**).

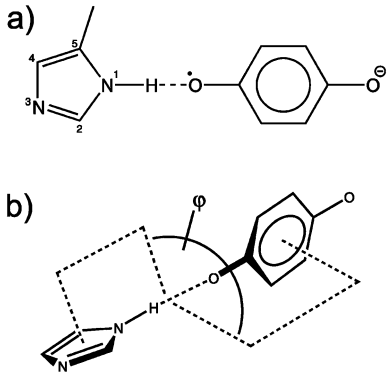

Fig. 4 Definition of the (a) atom numbering scheme and (b) twist angle φ for the methylimidazole–benzosemiquinone complexes.

† The Z-matrix was constructed using dummy atoms to allow the movement of the oxygen atom out of the imidazole ring plane. During optimization only the distance between O and a dummy atom but not between O and N was frozen.

Table 2 Theoretical ^{14}N QC parameters for various geometries of the methylimidazole–benzosemiquinone anion radical complex as calculated on the UB3PW91/6-31G(d) level of theory. All QC constants are in MHz, all distances in Å and all angles in degrees

Model	r(O–N)	α^a	β^a	φ	χ(N1)	η(N1)	χ(N3)	η(N3)
Q1	2.50	0	0	0	+1.482[b]	0.723	+3.722	0.061
Q2	2.75	0	0	0	+1.917	0.605	+3.751	0.052
Q3	3.00	0	0	0	+2.191	0.311	+3.775	0.044
Q4	3.25	0	0	0	+2.367	0.169	+3.791	0.037
Q5	3.00	20	0	0	+2.242	0.272	+3.780	0.048
Q6	3.00	0	25	0	+2.252	0.270	+3.812	0.056
Q7	3.00	20	32	0	+2.351	0.248	+3.810	0.072
Q8	3.00	0	0	45	+2.193	0.311	+3.773	0.044
Q9	3.00	0	0	90	+2.195	0.311	+3.773	0.044
Q10	3.00	16	32	45	+2.353	0.245	+3.806	0.070
Q11	2.50	20	33	0	+1.795	0.856	+3.745	0.081
MeIm[c]	—	—	—	—	+2.952	0.190	+3.920	0.016

[a] Due to the applied Z-matrix scheme where α and β are not directly included as variables or constants, the values differ slightly from model to model. [b] The largest component of the EFG tensor is not perpendicular to the imidazole ring here as in all other cases, *i.e.* V_{yy} and V_{zz} should be changed by definition. However, the corresponding coupling value of the perpendicular component is given to allow a comparison, even though the correct QC constant following the general definitions would be −1.720 MHz. [c] MeIm = Methylimidazole. Restricted Kohn–Sham calculation for the charge neutral state. The B3PW91/6-311+G(df,pd) level yields values of +2.789 MHz and 0.175 for N1 as well as +4.327 MHz and 0.115 for N3.

The influences on the EFG tensor are different for the four geometric parameters. Model **Q3** (r(O–N) = 3.00 Å, $\alpha = \beta = \varphi = 0°$) was taken as a reference model and all changes of the QC values are discussed with respect to this reference. In all cases the asymmetry parameter of N1 is the most sensitive value to changes of the hydrogen bond geometry.

The largest effect on η as well as on χ of the amino nitrogen is found for an alteration of the bond length. A shortening of this variable leads to a huge increase of the asymmetry parameter and a decrease of the QCC (**Q1** and **Q2**). When the hydrogen bond is elongated (**Q4**) an opposite change of the QC parameters is found – χ is increased and η is decreased. This is due to the fact that the smallest EFG tensor component V_{xx} which lies along the N–H bond becomes even smaller and the V_{yy} component increases when the bond is shortened. At the same time the V_{zz} component perpendicular to the ring plane decreases. In **Q1** this trend actually leads to a situation where the component perdendicular to the ring plane is no longer the largest and thus V_{yy} and V_{zz} change their directions by definition (see also Table 2). Upon distortion of the geometry by introducing an in- (**Q5**) or out-of-plane (**Q6**) angle a small increase of the QCC and a small decrease of the asymmetry parameter is observed for both. A combination of an in- and out-of-plane angle (**Q7**) leads to an effect which is almost the sum of each of the angle distortions alone. Both twist angles φ of 45° (**Q8**) and 90° (**Q9**) yield nearly the same QC parameters as the reference geometry **Q3**. As expected, the geometry with a combination of an in- and out-of-plane angle together with a twist angle $\varphi = 45°$ (**Q10**) possesses almost identical χ and η values as **Q7** where only α and β are non-zero but $\varphi = 0°$. The QC parameters of **Q11** with a short bond length of 2.50 Å as well as an in- and out-of-plane distortion reveal that the large effect of the hydrogen bond length (**Q1**–**Q4**) is still observable when the geometry is not planar and linear.

Based on the described trends a mapping of (χ, η) values onto certain specific hydrogen bond characteristics seems possible in a qualitative way. Smaller χ and larger η values than for the reference model **Q3** clearly indicate shorter hydrogen bonds, *i.e.* r(O–N) < 3.00 Å. Smaller η values in combination with larger χ values can be correlated with increased bond lengths and/or in- or out-of-plane distortions.

A closer look at the QC parameters of the imino nitrogen N3 from Table 2 shows that the influence of hydrogen bonding to N1 and alterations of the bonding geometry is much smaller than for the amino nitrogen – as expected for the remote nitrogen. Compared to free methylimidazole (see Table 2) the η(N3) values are always larger for the bound species and the χ(N3) values are smaller. A decrease of the bond length (**Q1**–**Q2**) and especially an additional out-of-plane distortion (**Q6**, **Q7**, **Q10** and **Q11**) have a small influence on the QC parameters of the remote imino nitrogen.

As was the case for the imidazole–water system a strong influence of the bonding situation of the amino nitrogen on its QC parameters can be found. Analysing these trends makes it possible to identify hydrogen bonding and also gain information about the geometry of this bond.

Application to biological systems

To test whether the results of this systematic study are transferable to quinones in biological systems, the available experimental QC and hydrogen bond geometry data for histidine residues involved in binding of semiquinone anion radicals $Q_A^{\bullet-}$ in bacterial reaction centres (bRCs)[45] and photosystem II (PSII)[46,47] was analysed and compared with some theoretical results from this work (Table 3). In this comparison only the hydrogen bond length was taken into account as this parameter has by far the strongest influence on the QC parameters. The experimental amino nitrogen ^{14}N QC parameters with values of χ = 1.56 – 1.65 MHz and η = 0.69 – 0.75 indicate hydrogen bond lengths shorter than 3.00 Å for all systems. Moreover, the calculated data from Table 2 suggests an intermediate hydrogen bond geometry somewhere between **Q1** (2.50 Å) and **Q2** (2.75 Å) which provides the closest agreement between theory and experiment for the QC constants as well as for the asymmetry parameters. The predicted O–N distance of 2.50–2.75 Å matches estimated values of about 2.5–2.7 Å for bRCs obtained from experimental hyperfine coupling constants (Table 3).[45] These distances were evaluated by comparison of the experimental hyperfine couplings with DFT calculations on model systems. For PSII the experimental values from EPR of 2.9(2) (F. MacMillan, personal communication) or 3.0(2) Å[48] are somewhat larger (see Table 3) but one has to take into account the uncertainties introduced by using the point-dipole approximation with estimated oxygen spin densities in these cases.‡ Crystallographic data yield larger distances of 2.9 Å for bRCs[28] and

‡ For a discussion of the reliability of distances derived from hyperfine or QC parameters for quinone model systems see *e.g.* refs. 22 and 49.

Table 3 Comparison of experimental hydrogen bond lengths and amino nitrogen QC parameters from histidine residues hydrogen-bound to semiquinone anion radicals in bacterial reaction centers (bRCs) and photosystem II (PSII) with calculated values from Table 2. All QC constants are in MHz and all distances in Å

Model/Biological system	r(O–N)	χ(N1)	η(N1)
Q1	2.50	+1.48	0.72
Q2	2.75	+1.92	0.61
$Q_A^{-\bullet}$–His219–Zn^{2+} in bRCs (*Rb. sphaeroides*)	2.5–2.7[a]	+1.65[a]	0.73
$Q_A^{-\bullet}$–His214–$Fe^{2+}_{(S=0)}$ in PSII	2.9(2)[b]	+1.65[c]	0.75
$Q_A^{-\bullet}$–His214–Zn^{2+} in PSII	3.0(2)[d]	+1.56[e]	0.69

[a] Distance and QC parameters from ref. 45, r(O–N) calculated from r(O–H) by adding a N–H bond length of 1 Å. [b] F. MacMillan, personal communication, calculated from r(O–H). [c] QC parameters from ref. 46. [d] Ref. 48, calculated from r(O–H) for a iron-depleted sample without Zn^{2+}. [e] QC parameters from ref. 47.

3.8 Å for PSII.[29] However, these values contain considerable uncertainties due to crystal structure resolutions of only 2.60 and 3.50 Å, respectively. Additionally, geometry optimisations for a large model of the $Q_A^{-\bullet}$ binding site in bRCs starting from a crystal structure model (unpublished data) as well as similar studies by O'Malley[50] show that the O–N bond length slightly decreases during the optimisation (by about 0.14–0.25 Å). Therefore, it can be concluded that the hydrogen bond lengths should be shorter for the semiquinone anion radical state in bRCs as well as in PSII than found in the available crystal structures.§ This was correctly predicted here by comparison of experimental QC values from the biological systems with the calculated QC parameters for the model systems in Table 2 and is in reasonable agreement with distance measurements by EPR.

It should be noted that the quantitative analysis of QC parameters in biological systems may be complicated by further influences from the surroundings, *e.g.* additional charged amino acids or metal ions might have an influence on the EFG and bonding situation of the amino nitrogen. In bRCs and PSII in most cases a divalent metal ion (Fe^{2+} or Zn^{2+}) is coordinated to the remote imino nitrogen of the histidine residue but in analogy to Jiang *et al.*[44] – who discussed that the amino ^{14}N QC parameters of Cu(II)-dien-*N*-benzylimidazole are comparable to those for solid *N*-benzylimidazole (not capable of forming hydrogen bonds at the amino position) as well as for imidazole in the gas phase – the effect of metal coordination at the imino position might not have a large impact on the amino nitrogen QC parameters. However, the presented application to semiquinone binding pockets in bRCs and PSII clearly demonstrates a more general validity of the trends found for the model systems in the systematic studies.

4. Conclusions

A systematic investigation of the influence of the hydrogen bond geometry on ^{14}N QC parameters for the model systems imidazole–water and methylimidazole–benzosemiquinone revealed a strong dependence on geometrical distortions of the bond and especially on the hydrogen bond length. χ and in particular η of the amino nitrogen have been shown to be sensitive probes to detect hydrogen bonding and additionally provide information about the hydrogen bond geometry. These results can in principle be used to determine the hydrogen bonding situation of histidines in biological systems. Histidine residues involved in hydrogen bonding to the amino nitrogen will in general possess smaller amino nitrogen QCCs and larger asymmetry parameters than free histidine or imidazole. Comparison of experimentally observed amino nitrogen QC parameters with the results of the systematic studies presented here (Fig. 2 and Table 2) may also help to gain further information about this bond, mainly about the bond length. The applicability of this procedure was demonstrated for the semiquinone binding pockets in bRCs and PSII.

This study provides a systematic insight into the sensitivity of quadrupole interaction parameters towards changes in the hydrogen bonding geometry and its findings may be used as an aid to interpret experimental ^{14}N quadrupole data involving hydrogen bonded imidazole derivatives or histidines in a qualitative way and relate them to geometric features of hydrogen bonds.

§ Sinnecker *et al.*[22] have demonstrated that the hydrogen bond between a benzoquinone and a water gets shorter by about 0.25 Å upon formation of the radical anion. This might also be of importance for comparison with crystal structures that probably involve neutral quinones.

Acknowledgements

This work was financially supported by the DFG (Sfb 472, *Molecular Bioenergetics*). J. F. gratefully acknowledges support by the Fonds der Chemischen Industrie (*Chemiefondsstipendium für Doktoranden*) and by the Frankfurt Center for Scientific Computing. Thanks to T. F. Prisner for his support and to F. MacMillan and M. Kobus for their help.

References

1 E. A. C. Lucken, *Nuclear Quadrupole Coupling Constants*, Academic Press, London, New York, 1969.
2 A. Schweiger and G. Jeschke, *Principles of Pulse Electron Paramagnetic Resonance*, Oxford University Press, Oxford, 1st edn., 2001.
3 A. Abragam, *The Principles of Nuclear Magnetism*, Oxford University Press, Oxford, New York, 1st edn., 1961.
4 R. G. Parr and W. Yang, *Density-Functional Theory of Atoms and Molecules*, Oxford University Press, New York, 1st edn., 1989.
5 A. M. Köster, P. Calaminici and N. Russo, *Phys. Rev. A*, 1996 **53**, 3865–3868.
6 R. Salzmann, M. Kaupp, M. T. McMahon and E. Oldfield, *J. Am. Chem. Soc.*, 1998, **120**, 4771–4783.
7 M. Torrent, D. G. Musaev, K. Morokuma, S.-C. Ke and K. J. Warncke, *J. Phys. Chem. B*, 1999, **103**, 8618–8627.
8 G. de Luca, N. Russo, A. M. Köster, P. Calaminici and K. Jug, *Mol. Phys.*, 1999, **97**, 347–354.
9 S.-C. Ke, M. Torrent, D. G. Museav, K. Morokuma and K. Warncke, *Biochemistry*, 1999, **38**, 12681–12689.
10 J. N. Latosińska and J. Koput, *Phys. Chem. Chem. Phys.*, 2000 **2**, 145–150.
11 M. Kaupp, C. Rovira and M. Parrinello, *J. Phys. Chem. B*, 2000, **104**, 5200–5208.
12 W. C. Bailey, *Chem. Phys.*, 2000, **252**, 57–66.
13 S. Dong, R. Ida and G. Wu, *J. Phys. Chem. A*, 2000, **104**, 11194–11202.
14 N. Nakamura, H. Masui and T. Ueda, *Z. Naturforsch., A*, 2000, **55a**, 315–322.
15 M. Torrent, D. Mansour, E. P. Day and K. Morokuma, *J. Phys. Chem. A*, 2001, **105**, 4546–4557.

16 E. Sicilia, G. de Luca, S. Chiodo, N. Russo, P. Calaminici, A. M. Köster and K. Jug, *Mol. Phys*., 2001, **99**, 1039–1051.
17 T. Janowski and M. Jaszunski, *Int. J. Quantum Chem*., 2002 **90**, 1083–1090.
18 J. N. Latosińska, *Int. J. Quantum Chem*., 2003, **91**, 284–296.
19 Y. Zhang, W. Gossman and E. Oldfield, *J. Am. Chem. Soc*., 2003, **125**, 16387–16396.
20 O. Schiemann, J. Fritscher, N. Kisseleva, S. T. Sigurdsson and T. F. Prisner, *ChemBioChem*, 2003, **4**, 1057–1065.
21 S. Gambarelli and J.-M. Mouesca, *Inorg. Chem*., 2004, **43**, 1441–1451.
22 S. Sinnecker, E. Reijerse, F. Neese and W. Lubitz, *J. Am. Chem. Soc*., 2004, **126**, 3280–3290.
23 G. A. Jeffrey and W. Saenger, *Hydrogen Bonding in Biological Structures*, Springer-Verlag, Berlin, New York, 1991.
24 A. Deacon, T. Gleichmann, A. J. Kalb (Gilboa), H. Price, J. Raftery, G. Bradbrook, J. Yariv and J. R. Helliwell, *J. Chem. Soc., Faraday Trans*., 1997, **93**, 4305–4312.
25 N. Ito, S. E. V. Phillips, K. D. S. Yadav and P. F. Knowles, *J. Mol. Biol*., 1994, **238**, 794–814.
26 B. C. Finzel, T. L. Poulos and J. Kraut, *J. Biol. Chem*., 1984, **259**, 13027–13036.
27 A. L. P. Houseman, P. E. Doan, D. B. Goodin and B. M. Hoffman, *Biochemistry*, 1993, **32**, 4430–4443.
28 M. H. B. Stowell, T. M. McPhillips, D. C. Rees, S. M. Soltis, E. Abresch and G. Feher, *Science*, 1997, **276**, 812–816.
29 K. N. Ferreira, T. M. Iverson, K. Maghlaoui, J. Barber and S. Iwata, *Science*, 2004, **303**, 1831–1838.
30 P. Nordlund, B.-M. Sjöberg and H. Eklund, *Nature*, 1990, **345**, 593–598.
31 S. Iwata, M. Saynovits, T. A. Link and H. Michel, *Structure*, 1996, **4**, 567–579.
32 G. W. Turner, R. L. Johnston and K. D. M. Harris, *Chem. Phys*., 2000, **256**, 159–168.
33 A. C. Saladino and S. C. Larsen, *J. Phys. Chem. A*, 2002, **106**, 10444–10451.
34 W. Gordy, *Theory and Applications of Electron Spin Resonance*, John Wiley & Sons, New York, 1st edn., 1980.
35 M. Tokman, D. Sundholm, P. Pyykkö and J. Olsen, *Chem. Phys. Lett*., 1997, **265**, 60–64.
36 P. Pyykkö, *Mol. Phys*., 2001, **99**, 1617–1629.
37 M. J. Frisch, G. W. Trucks, H. B. Schlegel, G. E. Scuseria, M. A. Robb, J. R. Cheeseman, V. G. Zakrzewski, J. Montgomery, R. E. Stratmann, J. C. Burant, S. Dapprich, J. M. Millam, A. D. Daniels, K. N. Kudin, M. C. Strain, O. Farkas, J. Tomasi, V. Barone, M. Cossi, R. Cammi, B. Mennucci, C. Pomelli, C. Adamo, S. Clifford, J. Ochterski, G. A. Petersson, P. Y. Ayala, Q. Cui, K. Morokuma, P. Salvador, J. J. Dannenberg, D. K. Malick, A. D. Rabuck, K. Raghavachari, J. B. Foresman, J. Cioslowski, J. V. Ortiz, A. G. Baboul, B. B. Stefanov, G. Liu, A. Liashenko, P. Piskorz, I. Komaromi, R. Gomperts, R. L. Martin, D. J. Fox, T. Keith, M. A. Al-Laham, C. Y. Peng, A. Nanayakkara, M. Challacombe, P. M. W. Gill, B. G. Johnson, W. Chen, M. W. Wong, J. L. Andres, C. Gonzalez, M. Head-Gordon, E. S. Replogle and J. A. Pople, *GAUSSIAN 98 (Revision A.11)*, Gaussian, Inc., Pittsburgh PA, 2001.
38 A. D. Becke, *J. Chem. Phys*., 1993, **98**, 5648–5652.
39 J. P. Perdew, *Physica B*, 1991, **172**, 1–6.
40 J. P. Perdew and Y. Wang, *Phys. Rev. B*, 1992, **45**, 13244 13249.
41 D. Christen, J. H. Griffiths and J. Sheridan, *Z. Naturforsch., A*, 1982, **37a**, 1378–1385.
42 M. L. S. Garcia, J. A. S. Smith, P. M. G. Bavin and C. R. Ganellin, *J. Chem. Soc., Perkin Trans. 2*, 1983, **9**, 1391–1399.
43 M. H. Palmer, F. E. Scott and J. A. S. Smith, *Chem. Phys*., 1983, **74**, 9–14.
44 F. Jiang, J. McCracken and J. Peisach, *J. Am. Chem. Soc*., 1990, **112**, 9035–9044.
45 W. Lubitz and G. Feher, *Appl. Magn. Reson*., 1999, **17**, 1–48.
46 Y. Deligiannakis, J. Hanley and A. W. Rutherford, *J. Am. Chem. Soc*., 1999, **121**, 7653–7664.
47 A. V. Astashkin, A. Kawamori, Y. Kodera, S. Kuroiwa and K. Akabori, *J. Chem. Phys*., 1995, **102**, 5583–5588.
48 F. MacMillan, F. Lendzian, G. Renger and W. Lubitz, *Biochemistry*, 1995, **34**, 8144–8156.
49 M. Flores, R. A. Isaacson, R. Calvo, G. Feher and W. Lubitz, *Chem. Phys*., 2003, **294**, 401–413.
50 P. J. O'Malley, *Chem. Phys. Lett*., 2003, **379**, 277–281.

